IJCSE International Journal of Computer Sciences and Engineering Open Access
Research Paper Vol-6, Special Issue-8, Oct 2018 E-ISSN: 2347-2693

Melanoma Skin Cancer Detection Using Improved RBF Classifier

K. Thenmozhi

Research Scholar, Dr.N.G.P Arts and Science College, Bharathiar University, Coimbatore, India

Available online at: www.ijcseonline.org

Abstract- Melanoma is a category of cancer that develops from the pigment-containing cells recognized as melanocytes. Melanomas usually ensue in the fur but may arise in the jaws, guts or ogle. This paper tends to two distinct frameworks for identification of skin growth in dermoscopy pictures. The primary framework utilizes worldwide strategies and the second framework utilizes neighborhood highlights and the classifier. Henceforth, melanoma is effortlessly to distinguish utilizing with help of worldwide strategies and neighborhood highlights. Skin Disease prediction has become important in a variety of applications such as health insurance, tailored health communication and public health. Due to the costs for dermatologists to monitor every patient, there is a need for an computerized system to evaluate a patient's risk of melanoma using images of their skin lesions captured using a standard digital camera. The traditional diagnosis technique aims at improving the quality of existing diagnostic systems by proposing advanced feature selection and classification methods.RBF neural network derives classification. For this classification (RBF neural network)this paper proposed new learning method using K means clustering. This paper focuses on the detection of skin lesion as a literature survey.

Keywords- Dermoscopy, Melanoma , Neural network, Clustering, Classification.

I.INTRODUCTION

Cancer has been characterized as a collection of related diseases involving abnormal cell growth with the potential to divide with- out stopping and spread into surrounding tissues. In Human, skin has complex surface, with fine scale geometry that makes its appearance difficult to model. Melanin and hemoglobin pigments are contained in this structure. Slight changes of pigment construction in skin may cause a rich variation in skin color.

Melanoma is one of the fastest growing cancers worldwide: Age-adjusted incidence rates have been increasing in most of the fair-skinned populations in recent decades; and 160,000 new cases are diagnosed annually worldwide (1–5). Melanoma is a malignancy of pigment-producing cells (melanocytes) located predominantly in the skin, but also found in the eyes, ears, GI tract, leptomeninges, and oral and genital mucous membranes. It can occur in any part of the body that contains melanocytes.

II. LITERATURE REVIEW

TaisiaHuckle et al (2014) described evaluated the consequences for strike rates of bringing down the base liquor acquiring age in New Zealand from 20 to 18 years .Estimated that the law change would expand strikes among youngsters matured 18 to 19 years (the objective gathering) and those matured 15 to 17 years through unlawful deals or liquor provided by more established companions or family membersUsing Poisson relapse, inspected end of the week ambushes bringing about hospitalization from 1995 to 2011. Results were surveyed independently by sexual orientation among youngsters matured 15 to 17 years and those matured 18 to 19 years, with those matured 20 and 21 years included as a control gathering.

Messadi M et al (2014)says the most recent years, PC vision-based determination frameworks have been generally utilized as a part of a few healing centers and dermatology facilities, pointing for the most part at the early recognition of threatening melanoma tumor, which is among the most incessant sorts of skin growth, versus different kinds of non-harmful cutaneous sicknesses. The death rate can be diminished by before discovery of suspicious sores and better avoidance. The point of this paper is to propose an interpretable grouping strategy for skin tumors in dermoscopic pictures in view of shape descriptors. This work introduces a fluffy govern based classifier to segregate a melanoma. A versatile Neuro Fuzzy induction System (ANFIS) is connected so as to find the fluffy guidelines prompting the right grouping.

Eduardo et al (2014)explained It is well known that alcohol impairs response inhibition and that adolescence is a critical period of neuromaturation where cognitive processes such as inhibitory control are still developing. In recent years, growing evidence has shown the negative consequences of alcohol binge drinking on the adolescent and young human brain. However,

the effects of cessation of binge drinking on brain function remain unexplored. The objective of the present study was to examine brain activity during response execution and inhibition in young binge drinkers in relation to the progression of their drinking habits over time. Event-related potentials (ERPs) elicited by a Go/NoGo task were recorded twice within a 2-year interval in 57 undergraduate students (25 controls, 22 binge drinkers, and 10 ex-binge drinkers) with no personal or family history of alcoholism or psychopathological disorders. The results showed that the amplitude of NoGo-P3 over the frontal region correlated with an earlier age of onset of regular drinking as well as with greater quantity and speed of alcohol consumption.

Angelina Pilatti et al (2013)proposed cancer is the second most important non-communicable disease worldwide and disproportionately impacts low- to middle-income countries. Diet in combination with other lifestyle habits seems to modify the risk for some cancers but little is known about South Americans. Food habits of Argentinean men pre- and post-diagnosis of prostate cancer (n = 326) were assessed along with other lifestyle factors. studied whether any of the behaviors and risk factors for prostate cancer were found in men with other cancers (n = 394), compared with control subjects (n = 629). Before diagnosis, both cases reported a greater mean consumption of meats and fats and lower intakes of fruits, green vegetables, cruciferous vegetables, legumes, nuts, seeds, and whole grains than the controls (all $p < 0.001$). After diagnosis, cases significantly reduced the intake of meats and fats, and reported other dietary modifications with increased consumption of fish, fruits (including red fruits in prostate cancer), cruciferous vegetables, legumes, nuts, and black tea (all $p < 0.001$).

Nadia Smaoui et al (2013)explainedIn recent years, there has been a fairly rapid increase in the number of melanoma skin cancer patients. Melanoma, this deadliest form of skin cancer, must be diagnosed early for effective treatment. So, it is necessary to develop a computer-aided diagnostic system to facilitate its early detection. In this paper, the proposed work is based on a combination of a segmentation method and an analytical method and aims to improve these two methods in order to develop an interface that can assist dermatologists in the diagnostic phase. As a first step, a sequence of preprocessing is implemented to remove noise and unwanted structures from the image. Then, an automatic segmentation approach locates the skin lesion. The next step is feature extraction followed by the ABCD rule to make the diagnosis through the calculation of the TDV score. In this research, three diagnosis are used which are melanoma, suspicious, and benign skin lesion. The experiment uses 40 images containing suspicious melanoma skin cancer. Based on the experiment, the accuracy of the system is 92% which reflects its viability

Teresa Mendonca (2013)says the increasing incidence of melanoma has recently promoted the development of computer-aided diagnosis systems for the classification of dermoscopic images. Unfortunately, the performance of such systems cannot be compared since they are evaluated in different sets of images by their authors and there are no public databases available to perform a fair evaluation of multiple systems. In this paper, a dermoscopic image database, called PH^2, is presented. The PH^2 database includes the manual segmentation, the clinical diagnosis, and the identification of several dermoscopic structures, performed by expert dermatologists, in a set of 200 dermoscopic images. The PH^2 database will be made freely available for research and benchmarking purposes.

Angel Alfonso Cruz-Roa et al (2013)focused and evaluate a deep learning architecture for automated basal cell carcinoma cancer detection that integrates (1) image representation learning, (2) image classification and (3) result interpretability. A novel characteristic of this approach is that it extends the deep learning architecture to also include an interpretable layer that highlights the visual patterns that contribute to discriminate between cancerous and normal tissues patterns, working akin to a digital staining which spotlights image regions important for diagnostic decisions. Experimental evaluation was performed on set of 1,417 images from 308 regions of interest of skin histopathology slides, where the presence of absence of basal cell carcinoma needs to be determined. Different image representation strategies, including bag of features (BOF), canonical (discrete cosine transform (DCT) and Haar-based wavelet transform (Haar)) and proposed learned-from-data representations, were evaluated for comparison. Experimental results show that the representation learned from a large histology image data set has the best overall performance (89.4% in F-measure and 91.4% in balanced accuracy), which represents an improvement of around 7% over canonical representations and 3% over the best equivalent BOF representation.

Mahmoud Elgamal et al (2013) described early detection of skin cancer has the potential to reduce mortality and morbidity. Two hybrid techniques for the classification of the skin images to predict it if exists. The proposed hybrid techniques consists of three stages, namely, feature extraction, dimensionality reduction, and classification. In the first stage, obtained the features related with images using discrete wavelet transformation. In the second stage, the features of skin images have been reduced using principle component analysis to the more essential features. In the classification stage, two classifiers based on supervised machine learning have been developed. The first classifier based on feed forward back-propagation artificial neural network and the second classifier based on k-nearest neighbor. The classifiers have been used to classify subjects as normal or

abnormal skin cancer images. A classification with a success of 95% and 97.5% has been obtained by the two proposed classifiers and respectively. This result shows that the proposed hybrid techniques are robust and effective.

Ravi Kumar et al (2013)proposed breast cancer is one of the major causes of death in women when compared to all other cancers. Breast cancer has become the most hazardous types of cancer among women in the world. Early detection of breast cancer is essential in reducing life losses. This paper presents a comparison among the different Data mining classifiers on the database of breast cancer Wisconsin Breast Cancer (WBC), by using classification accuracy. This paper aims to establish an accurate classification model for Breast cancer prediction, in order to make full use of the invaluable information in clinical data, especially which is usually ignored by most of the existing methods when they aim for high prediction accuracies.

Kawsar Ahmed et al (2014) explain lung cancer is the leading cause of cancer death worldwide Therefore, identification of genetic as well as environmental factors is very important in developing novel methods of lung cancer prevention. However, this is a multi-layered problem. Therefore a lung cancer risk prediction system is here proposed which is easy, cost effective and time saving. Materials and methods: Initially 400 cancer and non-cancer patients' data were collected from different diagnostic centres, pre-processed and clustered using a K-means clustering algorithm for identifying relevant and non-relevant data. Next significant frequent patterns are discovered using AprioriTid and a decision tree algorithm. Results: Finally using the significant pattern prediction tools for a lung cancer prediction system were developed. This lung cancer risk prediction system should prove helpful in detection of a person's predisposition for lung cancer. Conclusions: Most of people of Bangladesh do not even know they have lung cancer and the majority of cases are diagnosed at late stages when cure is impossible.

III. PROPOSED METHODOLOGY

Feature selection

Pearson's correlation coefficient when applied to a population is commonly represented by the Greek letter ρ (rho) and may be referred to as the *population correlation coefficient* or the *population Pearson correlation coefficient*. The formula $\rho$for is:

$$\rho X, Y = \frac{cov(X,Y)}{\sigma_X \sigma_Y}$$

Where:

- Cov is the covariance
- σ_X is the standard deviation of X
- σ_Y is the standard deviation of Y

The formula for ρ can be expressed in terms of mean and expectation. Since
Cov(X,Y) = E[(X – μ_X)(Y –μ_Y)],
The formula for ρ can also be written as

$$\rho_{X,Y} = \frac{(E[(X-\mu X)(Y-\mu Y)])}{\sigma_X \sigma_Y}$$

Where:

- Cov and σ_X are defined as above
- μ_X is the mean of X
- E is the expression

Centered based RBF

A set of N training data points in a D dimensional input space, such that each input vector $\mathbf{x}_p = \{xip: i = 1,...,D\}$ has a corresponding K dimensional target output $\mathbf{t}$ $p = \{t_k^p: k = 1,...,K\}$.The target outputs will generally be generated by some underlying functions $g_k(\mathbf{x})$ plus random noise. The goal is to approximate the $g_k(\mathbf{x})$ with functions $y_k(\mathbf{x})$ of the form

$$Y_k(X) = \sum_{j=0}^{M} w_{kj} \emptyset_j (X)$$

We shall concentrate on the case of Gaussian basis functions

$$\emptyset_j(x) = \exp\left(-\frac{\|X-\mu_j\|^2}{2\sigma_j^2}\right)$$

which have centres $\{\mu j\}$ and widths $\{\sigma j\}$. Naturally, the way to proceed is to develop a process for finding the appropriate values for M, $\{wkj\}$, $\{\mu ij\}$ and $\{\sigma j\}$.

The RBF Mapping can be cast into a form that resembles a neural network

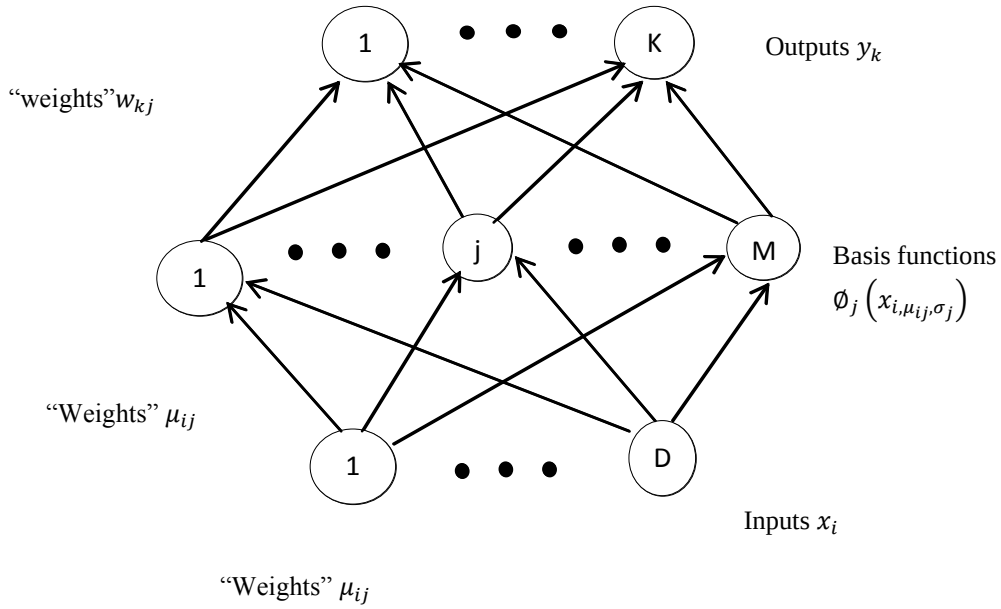

The hidden to output layer part operates like a standard feed-forward MLP network, with the sum of the weighted hidden unit activations giving the output unit activations. The hidden unit activations are given by the basis functions φ *j* (**x**,μ*j* ,σ *j*), which depend on the "weights" {μ*ij*,σ *j*} and input activations {*xi*} in a non-standard manner.

One major advantage of RBF networks is the possibility of determining suitable hidden unit/basis function parameters without having to perform a full non-linear optimization of the whole network.

Learning layer
For setting the RBF parameters is to have their centres fixed at *M* points selected from the *N* data points, and to set all their widths to be equal and fixed at an appropriate size for the distribution of data points.

Initially, for each class C, find $S_i=\{X_i\}$, where class(X_i)∈C_j . Apply K-means clustering using jaccard index distance to each class to S and extract two clusters from S. Cluster containing n vectors δi={V_1….V_n} .Select V_i,V_j which has max d_{ij}. d_{ij}=distance(V_i,V_j) i,j∈1,2… n . Update center list ⊖⇐⊖∪{V_i,V_j}.

The K-means clustering algorithm uses iterative refinement to produce a final result. The algorithm inputs are the number of clusters K and the data set. The data set is a collection of features for each data point. The algorithms starts with initial estimates for the K centroids, which can either be randomly generated or randomly selected from the data set. The algorithm then iterates between two steps:

1. Data assignment step:
Each centroid defines one of the clusters. In this step, each data point is assigned to its nearest centroid, based on the squared Euclidean distance. More formally, if ci is the collection of centroids in set C, then each data point x is assigned to a cluster based onJaccard index.

The Jaccard index, also known as Intersection over Union and the Jaccard similarity coefficient is a statistic used for comparing the similarity and diversity of sample sets. The Jaccard coefficient measures similarity between finite sample sets, and is defined as the size of the intersection divided by the size of the union of the sample sets:

$$J(A,B) = \frac{|A \cap B|}{|A \cup B|} = \frac{|A \cap B|}{|A| + |B| - |A \cap B|}$$

wheredist(·) is the jaccard distance. Let the set of data point assignments for each ith cluster centroid be Si.

2. Centroid update step:
In this step, the centroids are recomputed. This is done by taking the mean of all data points assigned to that centroid's cluster.

$$c_{i=\frac{1}{|S_i|}}\sum x_{i\epsilon s_i^{x_i}}$$

The algorithm iterates between steps one and two until a stopping criteria is met (i.e., no data points change clusters, the sum of the distances is minimized, or some maximum number of iterations is reached).

This algorithm is guaranteed to converge to a result. The result may be a local optimum (i.e. not necessarily the best possible outcome), meaning that assessing more than one run of the algorithm with randomized starting centroids may give a better outcome.

Choosing K
The algorithm described above finds the clusters and data set labels for a particular pre-chosen K. To find the number of clusters in the data, the user needs to run the K-means clustering algorithm for a range of K values and compare the results. In general, there is no method for determining exact value of K.

One of the metrics that is commonly used to compare results across different values of K is the mean distance between data points and their cluster centroid. Since increasing the number of clusters will always reduce the distance to data points, increasing K will always decrease this metric, to the extreme of reaching zero when K is the same as the number of data points. Thus, this metric cannot be used as the sole target. Instead, mean distance to the centroid as a function of K is plotted and the "elbow point," where the rate of decrease sharply shifts, can be used to roughly determine K.

A number of other techniques exist for validating K, including cross-validation, information criteria, the information theoretic jump method, the silhouette method, and the G-means algorithm. In addition, monitoring the distribution of data points across groups provides insight into how the algorithm is splitting the data for each K.

Algorithm
Learning process of centers in RBF
Input: $X = \{X1, X2 \ldots XN\}$ is set of samples
$C = \{C1 \ldots . Ck\}$ //set of classes
$X_i=[x_{i1},x_{i2},x_{i3} \ldots x_{ip}]$ denotes p-dimension vector of training set in each sample
Output: $\ominus = \{\}$ //Center list initially empty
Step 1: For each class Ci

$$Si = \{Xi\}$$

where class(X_i)$\in C_j$
Step 2: Apply K-means clustering using Jaccard Index distance to S_i
Extract 2 cluster$\{\delta 1, \delta 2\}$ from Si;
Step 3: //cluster containing n vectors
For i= 1 to 2
$\delta i = \{V1 \ldots . Vn\}$
Select V_i,V_j which has max d_{ij}. d_{ij}=distance(Vi, Vj) $i, j \in 1,2 \ldots n$ //distance() is Euclidean distance
Update center list $\ominus \Leftarrow \ominus \cup \{Vi, Vj\}$.
End for
Step 4: End for;
Output: $\ominus$ selected centers for RBF Network

Weighted layer

The equations for the weights are most conveniently written in matrix form by defining matrices with components.

$$\emptyset^{\mathrm{T}}(\mathrm{T} - \emptyset \mathrm{w}^{\mathrm{T}})$$

And hence te formal solution for the weights is

$$W^T = (\emptyset^T \emptyset)^{-1} \emptyset^T T = \emptyset^{\dagger} T$$

This involves the standard pseudo-inverse of $\emptyset$ which is defined as
$\emptyset^{\dagger} = (\emptyset^T \emptyset)^{-1} \emptyset^T \equiv$

And can be seen to have the property $\emptyset^{\dagger}\emptyset = \mathrm{I}$.
Thus the network weights can be computed by fast linear matrix inversion techniques.

Output layer
Since the hidden unit activations φj (**x**,μj ,σj) are fixed while the output weights $\{w_{jk}\}$ are determined, we essentially only have to find the weights that optimize a single layer linear network.

$$E = \frac{1}{2}\sum_{p}\sum_{k}\left(t_k^p - y_{k(x^p)}\right)^2$$

And here the outputs are a simple linear combination of the hidden unit activations, i.e $y_k(x^p) = \sum_{j=0}^{M} w_{kj\emptyset_j}(x^p)$.
At the minimum of E the gradients with respect to all weights w_{kj} will be zero, so

$$\frac{\boldsymbol{\partial E}}{\boldsymbol{\partial w_{kj}}} = \sum_{\boldsymbol{p}}\left(\boldsymbol{t_k^p} - \sum_{\boldsymbol{j=0}}^{\boldsymbol{M}} \boldsymbol{w_{kj}}\,\emptyset_{\boldsymbol{j(X^p)}}\right)\emptyset_{\boldsymbol{i}}(\boldsymbol{X^p}) = \mathbf{0}$$

And linear equations like this are well known to be easy to solve analytically.

$$\rho X, Y = \frac{cov(X,Y)}{\sigma_x \sigma_y}$$

Where :

- Cov is the covariance
- σ_X is the standard deviation of X
- σ_Y is the standard deviation of Y

The formula for ρ can be expressed in terms of mean and expectation. Since

$$\mathrm{Co}v(X,Y) = E[(X-\mu_X)(Y-\mu_Y)]$$

The formula for ρ can also be written as

$$\rho X, Y = \frac{E[(X-\mu_X)(Y-\mu_Y)]}{\sigma_X \sigma_Y}$$

IV. EXPERIMENTAL RESULTS

The proposed system can be evaluated using various data sets taken from different sources in the internet. The Leprosy Skin cancer, skin data set is taken from BIOGPS (http://biogps.org/dataset/tag/skin/), national cancer data set, gene data set, non-melanoma cancer data set, lesion skin data set are taken from NCBI repository http://www.ncbi.nlm.nih.gov/. The performances of the proposed techniques are evaluated for the skin cancer. The proposed techniques performance evaluated in terms of sensitivity, specificity, precision, execution time, F-measure and accuracy.

The above performances are evaluated using following parameters:
TP (True Positive): Malignant Melanoma data that are correctly classified by the classifier. FP (False Positive): Non-cancer data Normal regions that are wrongly classified as Malignant Melanoma by the classifier.TN (True Negative): Non-cancer data that are correctly classified by the classifier. FN (False Negative): Malignant Melanoma data that are wrongly classified as Non-cancer data by the classifier.

Table 1: Comparison of performance metrics between classifiers using PCA features

Metrics	kNN classifier	SOM	SVM	Proposed Improved RBF ANN classifier
Sensitivity	84%	85.71%	85%	98.09%
Specificity	84%	87%	84%	95.83%
Accuracy	88%	86.04%	89.5%	98%
Precision	86.5%	87%	87%	99%
F-measure	89.3	90.45%	89.35	98.56

Table 2: Comparison of performance metrics between classifiers using LDA features

Metrics	kNN classifier	SOM	SVM	Proposed Improved RBF ANN classifier
Sensitivity	74.28%	81.90	79.04	91.42%
Specificity	79	78.65	78.65	79.16%
Accuracy	75.19%	81.39	79.06	89.14%
Precision	93.97%	95	94.31	95.04%
F-measure	82.53%	87.75	85.56	93.3%

Table 3: Comparison of performance metrics between classifiers using combination of PCA and LDA features

Metrics	kNN classifier	SOM	SVM	Proposed Improved RBF ANN classifier
Sensitivity	80.9	83.80	80.70	93.3%
Specificity	83.56	87	83.56	83.3%
Accuracy	81.39	84.49	81.39	91.47
Precision	87%	96.70%	87.62%	97.02%
F-measure	87.62%	89.79%	88.54%	95.14%

The table 1-3 shows the comparison of sensitivity between kNN, SVM, SOM and proposed improved RBF ANN classifier using three features such as PCA, LDA and combination of PCA and LDA algorithm. Totally 259 skin cancer data are collected from given dataset where 129 skin cancer data are collected as testing purpose in which 105 data are affected by melanoma skin cancer and remaining 24 skin cancers are non-melanoma. The performance metrics of sensitivity and specificity are calculated using TP, FN, TN and FP parameters. The TP and FN parameter is used to calculate the sensitivity where 78 and 28 for kNN classifier using PCA features, for SVM classifier is 83 and 22, 86 and 19 for SOM classifier, TP is 96 and FN is 9 for improved RBF ANN classifier. In the case of specificity using PCA features, TN and FP parameters are used in which 19 and 5 for kNN classifier, 19 and 5 for SVM classifier, 20 and 4 for SOM classifier, TN is 20 and FP is 4 for improved RBF kNN classifier.

The performance metrics of different classifier using LDA features are given in table 2. The TP and FN parameters of LDA features are 85 and 20 for kNN classifier, 85 and 20 for SVM classifier, 88 and 17 for SOM classifier, 98 and 7 for improved RBF ANN classifier. In case of specificity, TN and FP parameter is used. In which 20 and 4 for kNN classifier, 21 and 3 for SVM classifier, 20 and 4 for SOM classifier, 20 and 4 for improved RBF ANN classifier.

The performance metrics of different classifier using combination of PCA and LDA features are given in table 3. The TP and FN parameters of combination of PCA and LDA features are 88 and 19 for kNN classifier, 90 and 15 for SVM classifier, 90 and 15 for SOM classifier, 103 and 2 for improved RBF ANN classifier. In case of specificity, TN and FP parameter is used. In which 20 and 4 for kNN classifier, 20 and 4 for SVM classifier, 21 and 3 for SOM classifier, 23 and 1 for improved RBF ANN classifier. From the above table observed that improved RBF ANN classifier provides better performance compared to other approaches. The classifier provides better performances using LDA features.

V. CONCLUSION

So as to accomplish better precision in the forecast of maladies, enhancing survivability rate with respect to genuine passing related issues and so on different information mining strategies must be utilized as a part of mix. Achieve better classification by using improved RBF neural network. To accomplish therapeutic information of higher quality all the vital advances must be taken keeping in mind the end goal to construct the better medicinal data frameworks which gives exact data in regards to patients restorative history as opposed to the data with respect to their charging solicitations. Since fantastic social insurance information is helpful for giving better therapeutic administrations just to the patients yet in addition to the medicinal services associations or whatever other associations who are engaged with human services industry.

REFERENCES

[1]. TaisiaHuckle, and Karl Parker, Long-Term Impact on Alcohol-Involved Crashes of Lowering the Minimum Purchase Age in New Zealand, American Journal of Public Health, Vol. 104, pp.1087-1091,June 2014.

[2]. Messadi M, Ammar M, Cherifi H, Chikh MA and Bessaid A," Interpretable Aide Diagnosis System for Melanoma Recognition", 2014, Bioengineering & Biomedical Science.

[3]. Eduardo López-Caneda, Socorro Rodríguez Holguín, Montserrat Corral, Sonia Doallo, Fernando Cadaveira, Evolution of the binge drinking pattern in college students: Neurophysiological correlates, Alcohol (Elsevier) Vol. 48 , 2014.

[4]. Angelina Pilatti , Juan Carlos Godoy , SilvinaBrussino , Ricardo Marcos Pautassi," Underage drinking: Prevalence and risk factors associated with drinking experiences among Argentinean children", Alcohol(Elsevier), Vol. 47, pp. 323- 331, 2013.

[5]. Nadia Smaoui, SouhirBessassi," A developed system for melanoma diagnosis",2013, International Journal of Computer Vision and Signal Processing, 3(1), 10-17(2013).

[6]. Teresa Mendonca, Pedro M. Ferreira,Jorge S. Marques, Andre R. S. Marcal, Jorge Rozeira," PH2 - A dermoscopic image database for research and benchmarking",2013, 35th Annual International Conference of the IEEE EMBS Osaka, Japan, 3 - 7 July, 2013.

[7]. Angel Alfonso Cruz-Roa, John Edison ArevaloOvalle, AnantMadabhushi, and Fabio Augusto Gonz´alez Osorio," A Deep Learning Architecture for Image Representation, Visual Interpretability and Automated Basal-Cell Carcinoma Cancer Detection",2013.

[8]. Mahmoud Elgamal ," AUTOMATIC SKIN CANCER IMAGES CLASSIFICATION", 2013, (IJACSA) International Journal of Advanced Computer Science and Applications, Vol. 4, No. 3, 2013.

[9]. G. Ravi Kumar, Dr. G. A. Ramachandra, K.Nagamani," An Efficient Prediction of Breast Cancer Data using Data Mining Techniques", International Journal of Innovations in Engineering and Technology (IJIET),Vol. 2 ,No. 4, pp139- 144, August 2013.

[10]. Kawsar Ahmed, Abdullah Al Emran, TasnubaJesmin, Roushney Fatima Mukti,MdZamilurRahman, Farzana Ahmed," Early Detection of Lung Cancer Risk Using Data Mining", Asian Pacific Journal of Cancer Prevention, Vol. 14,pp. 595- .2014

